Size Dependence of 1D Superconductivity in NbN Nanowires on Suspended Carbon Nanotubes

T. Hashimoto, N. Miki, and H. Maki

Abstract—We report the size dependence of 1D superconductivity in ultrathin (10-130 nm) nanowires produced by coating suspended carbon nanotubes with a superconducting NbN thin film. The resistance-temperature characteristic curves for samples with 25 nm wire width show the superconducting transition. On the other hand, for the samples with 10-nm width, the superconducting transition is not exhibited owing to the quantum size effect. The differential resistance vs. current density characteristic curves show some peak, indicating that Josephson junctions are formed in nanowires. The presence of the Josephson junctions is well explained by the measurement of the magnetic field dependence of the critical current. These understanding allow for the further expansion of the potential application of NbN, which is utilized for single photon detectors and so on.

Keywords—NbN nanowire, carbon nanotube, quantum size effect, Josephson junction.

I. INTRODUCTION

SUPERCONDUCTING nanowires have been the subject of intense experimental studies these past few years on both applied and fundamental levels. On the applied level, these systems appear to be adequate devices for photon detection [1], reaching the single photon detection threshold [2]. Photon detectors based on ultrathin nanowires are expected to efficiently detect mid-infrared photons and to operate at low bias currents [3]. On the fundamental level, a technique that employs suspended single-wall carbon nanotubes (CNTs) as nanowire templates for material deposition has been developed [4],[5]. Because of the small diameter (1-2 nm) and the chemical stability of CNTs, this technique makes it possible to prepare the nanowires with a wide variety of materials. This technique is of practical importance for the small systems, such as ultrathin nanowires, or Josephson junctions which is made by sandwiching a thin layer of a non-superconducting material between two layers of superconducting material. The technique was originally used to obtain sub-10 nm wires of a superconducting amorphous Mo-Ge alloy [4], [6], [7]. Later, it was found that continuous nanowires–Au, Pd, Fe, Al and Ti-can also be formed [8]. However, NbN ultrathin nanowires on suspended CNTs has not been reported so far. In recent years, NbN has been well studied owing to its very high transition temperature T_c, high hardness, melting point, wear resistance [9], chemical inertness [10] and temperature stability [11]. Therefore, among superconducting nanowires, the technology based on NbN ultrathin films appeared to be very promising route and has been favored for the implementation of single photon detectors [1]-[3].

In this paper, we report on the experimental study of NbN ultrathin (10-130 nm) nanowires on suspended CNTs by four terminal electrometric method. We observed the superconductor – insulator transition in the W=10-nm nanowire and the some peaks at the differential resistance which are the unique features of the Josephson junctions.

II. EXPERIMENTAL PROCEDURE

We prepared nanowires and thin films for comparison. NbN films were deposited by radio frequency magnetron sputtering of Nb in Ar and N_2 plasma at the condition of RF power of 70 W, N_2 gas concentration of 2 %, gas pressure of 0.4 Pa and substrate temperature of 350 K on a quartz substrate. The film thickness was 130nm. The nanowires were fabricated as follow. The Si substrate was covered with a 120 nm-layer of SiO_2. Slits were patterned in the SiO_2 film using electron beam lithography and dry etching and the widths of those are 1-5 μm. The Si layer under slits was removed using dry etching to form an undercut structure. The CNTs suspended over the slits were grown by chemical vapor deposition and NbN was subsequently sputtered on the CNTs, as in Fig. 1a. b. The sputtering conditions were the same as thin films for comparison. The wire-widths W are 10 , 25 , 30 , 40 , 50 , 60 , 90 , 130 nm (estimated from the deposition time and the image of scanning electron microscope : SEM).
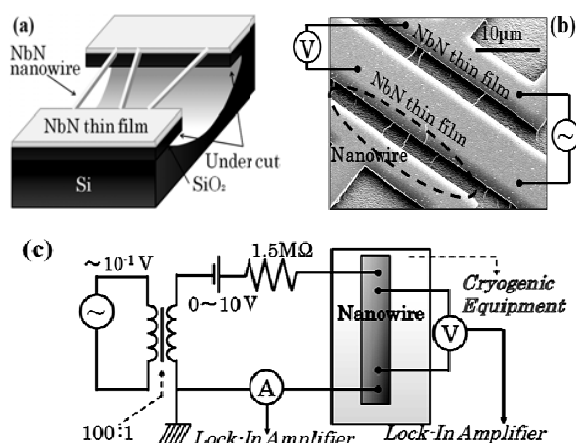

Fig. 1 The device architecture and the measurement system. (a) The device schema. (b) SEM image of the device. (c) The measurement system by four terminal electrometric method at low temperature

T. Hashimoto is with Maki Laboratory, Keio University, 3-14-1 Hiyoshi, Kohoku-ku, Yokohama-shi, Kanagawa-ken, Japan (phone: 045-566-1643; fax: 045-566-1587; e-mail: hashimoto@ az.appi.keio.ac.jp).

N. Miki is with Miki Laboratory, Keio University, 3-14-1 Hiyoshi, Kohoku-ku, Yokohama-shi, Kanagawa-ken, Japan (e-mail: miki@mech.keio.ac.jp).

H. Maki is with Maki Laboratory, Keio University , 3-14-1 Hiyoshi, Kohoku-ku, Yokohama-shi, Kanagawa-ken, Japan (e-mail: maki@appi.keio.ac.jp).

The crystal structure, magnetization and electric properties of the NbN film (thickness: 130 nm) on SiO_2 were investigated by $2\theta/\theta$ x-ray diffraction (XRD) and superconducting quantum interference device (SQUID) and the four-probe electric measurements at low temperature (2.9-20.0 K), respectively. The electric properties of the wires were investigated by the four-probe electric measurements at low temperature (2.9-20.0 K), as in Fig. 1b, c. The four probes were formed by wire-bonding a pair of wires onto NbN contact pad. The critical temperature (T_c) of the films and nanowires were estimated from to the resistance-temperature (R-T) characteristic curves at low alternating current, which is a few nA far below the critical current (I_c). The critical current density (J_c) of the nanowires was estimated from the differential resistance (dV/dI)-density current characteristic curves at low alternating current and variable direct current. In addition, in W=40-nm nanowire, the magnetic field dependence of I_c was obtained by applied magnetic field to the above measurement system. The detection of the applied magnetic field was perpendicular to the axial direction of nanowires.

III. RESULT AND DISCUSSION

Fig. 2 (a) shows the XRD pattern of the 130-nm thick NbN film. The XRD pattern of the film includes some peaks which correspond to NbN. Fig. 2 (b) shows the magnetic field dependence of the magnetization. The upper critical field H_{c2} is ~10 MA/m. The coherence length ξ is estimated to be 162 nm by using

$$H_{c2} = \phi_0 / 2\pi\xi^2 , \qquad (1)$$

Where magnetic-flux quantum ϕ_0=2.07×10^{-15} Vs. The coherence length is one of the important parameter characterizing the phenomenon of superconductivity in a
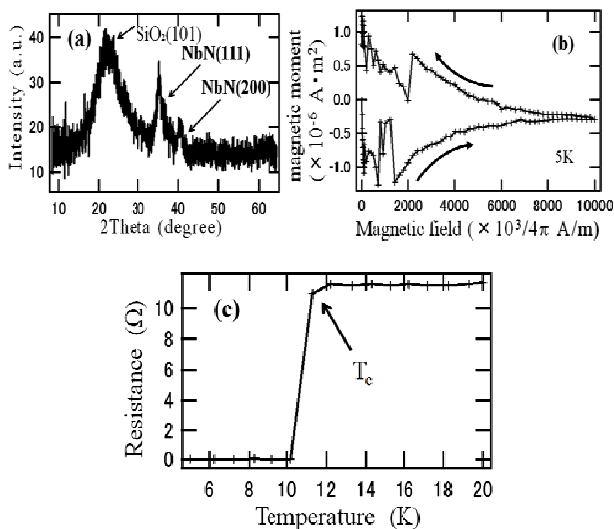

Fig. 2 The superconductivities of 130-nm thickness NbN film. (a) XRD pattern. (b) magnetic field dependence at 5 K. (c) R-T curve of the film
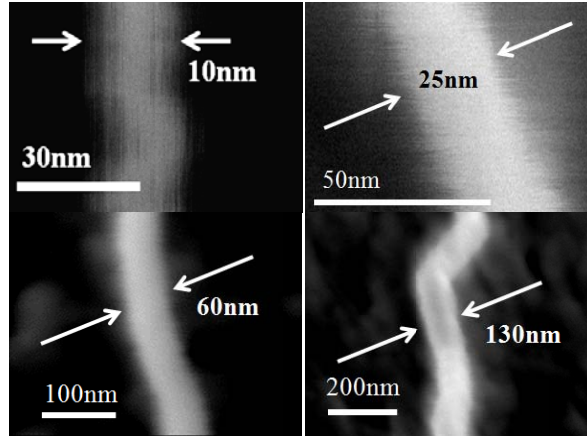

Fig. 3 SEM images of the NbN nanowire on a suspended CNT

low-dimensional superconductor, which is equal to the length of spatially varying the superconducting order parameter. When the coherence length is long, the wire is resistant to defects. When the coherence length is short, the wire is sensitive to defects. ξ=162 nm is long enough in comparison with the diameter of wires, which implies the wire is resistant to defects such as grain boundaries. In addition, when this parameter becomes comparable to, or large than, the device dimensions, the quantum size effects occur [4], [12], [13]. Therefore, it is expected that the quantum size effects appear if the wire-width in the device is close to the coherence length. Fig. 2 (c) shows the R-T characteristic curve of the NbN film. The superconducting transition is T_c = 12.0 K, where T_c are defined as 90 % $R_{(20K)}$. When the wire-width is close to the coherence length, the superconducting fluctuation occurs.

Fig. 3 shows the SEM images of the NbN nanowire on the suspended CNT. The NbN nanowires close to the desired wire width are fabricated, corresponding to the film thickness estimated form the sputtering time.

Fig. 4a shows the R-T characteristic curves for the NbN nanowires, which is normalized at the resistance at 20 K. For thicker nanowires than W=25-nm, the R-T curves show the resistance drop with cooling, indicating the superconducting transition. However, for W=10-nm nanowire, the R-T curve does not show the superconducting transition, i.e., the resistance stays almost constant with cooling. Therefore, the nanowire may be normal or even insulating material. In fact, it should be considered insulating because the resistance increases at low enough temperatures [14]. On the other hand, the 10-nm thickness film shows the superconducting transition at around 8 K (Fig. 4b). These results imply the occurrence of the quantum size effect in NbN nanowire. Reference [15] shows the model of the superconductor-insulator transition. This model is the ideal that the superconductor-insulator transition occurs by fluctuations in the phase of the order parameter even though the amplitude remains finite. The superconducting phase is considered to be a condensate Cooper pairs with localized vortices, while the insulating phase is a condensate of vortices with localized Cooper pairs. In this model, the nanowires can become superconducting or

insulating depending on the ratio of their normal state resistance (R_N) to the quantum resistance for Cooper pairs ($R_q =$
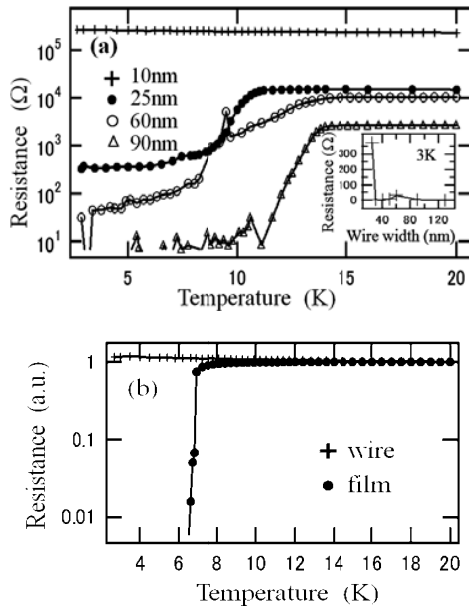

Fig. 4 (a) The *R-T* characteristic curves of the nanowires. Inset: Residual resistance of nanowires at 3 K. (b) The *R-T* characteristic curves of the 10-nm thickness film and *W*=10-nm nanowire

$h/(2e)^2 = 6.45$ kΩ). Reference [16] shows that the values of R_N/R_q separated into superconducting and insulating properties indicate from 0.85 to 2.9. The results of our measurement on nanowires show the superconducting transition for *W* 25-nm nanowires, R_N/R_q of which indicates below 2.3, and the superconducting properties become stronger when R_N/R_q increases. In contrast to this, that of *W*=10-nm nanowire indicates 35, which shows the insulator properties. Although the superconductor-insulator transition occurs at $R_N/R_q > 2.3$, it is necessary to investigate more closely.

Focusing on the residual resistance at 3 K, the major change appears in that for *W*=25-nm nanowire (The inset of Fig. 4a). Whereas the residual resistance of $W \geqq 30$-nm nanowires is about several ohm or a significantly lower resistance which can be locked by the lock-in-amplifier, the residual resistance of *W*=25-nm nanowire is above 350 Ω. The size effect can also be observed in the transition temperature T_c. Whereas the T_c of $W \geqq 30$-nm nanowires is about 12 K, the T_c of *W*=25-nm nanowire is about 10 K. This is attributed to the fact that as the device dimension is close to 1D, quantum size effect begins to appear in the wire due to the superconducting fluctuation. In the *W*=10-nm wire, the superconductor–insulator transition appears in the wire by localized Cooper pairs.

Fig. 5(a) shows the differential resistance-current density characteristic curves of the *W*=30-nm nanowire. In the calculation of the current density, the cross section area of the nanowire is estimated from sputtering time and the SEM image. The critical current density for the 30-nm nanowire is $J_c \approx 2 \times 10^{12}$ A/m². After some peaks are appeared in the nanowire

at the differential resistance over the critical current density J_c, the differential resistance converges. This indicates that the I-V characteristic curve is expected to exhibit some voltage steps, which may be a phenomenon that is observed mostly in Josephson junctions. Underlying this phenomenon is
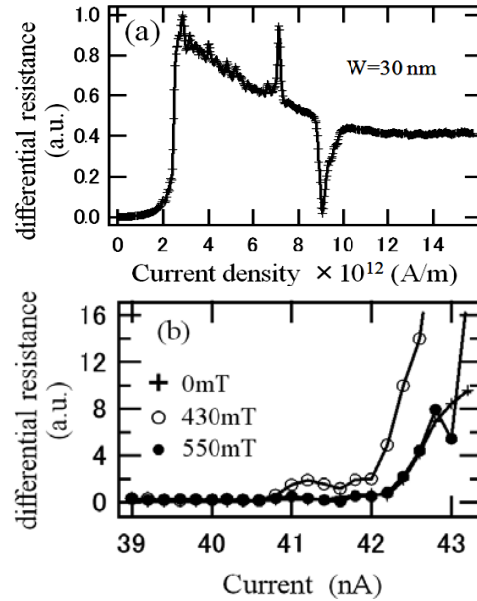

Fig. 5 (a) The differential resistance-current density characteristic curves of the *W*=30 nm nanowire. (b) The magnetic field dependence of the critical current of the *W*=40-nm nanowire

the picture of multiple Andreev reflections (MARs). An electron in a normal system slightly above the Fermi level is reflected back as a hole at one super conductor-normal system (NS) interface leaving a Cooper in the superconductor. The hole is reflected again as an electron at the other NS interface, and these processes are repeated coherently, resulting in a resonance-like behavior. The MAR is the hallmark of phase-coherent transport of Cooper pairs in mesoscopic Josephson junctions [17]. MARs and coherent Cooper pair transport have been observed mostly in Josephson junctions with semiconductor or semimetal as a normal system [18]-[20].

On the other hand, as a phenomenon observed in a Josephson junction system, the change of the critical current I_c should be observed under applying magnetic field as reported in Reference [21]. Fig. 5b shows the differential resistance-current density characteristic curves in magnetic fields of the *W*=40-nm nanowire, in which the peak shift, that is, the critical current modification, is observed. This shows the subsistent of Josephson junctions. The Josephson junctions in our NbN nanowire might originate from the fluctuation of the NbN composition or the existence of grain boundaries owing to the thinly deposition on 1D CNTs.

IV. CONCLUSION

We prepared the ultrathin NbN superconducting nanowire on the suspended CNTs, and have discussed the size effect of the

superconducting properties in the 1D NbN. W=10-nm nanowire shows the superconductor–insulator transition, and W=25-nm nanowire begins to show the superconducting fluctuation. From the differential resistance-current density characteristic curves, the signatures of the Josephson junction are observed. We anticipate that NbN nanowire on the suspended CNTs will provide more applications involving single photon detectors.

REFERENCES

[1] R. H. Hadfield, "Single-photon detectors for optical quantum information applications," *Nat. Photonics*, vol. 3, pp. 696−705, Nov. 2009.

[2] G. N. Gol'tsman, O. Okunev, G. Chulkova, A. Lipatov, A. Semenov *et al.*, "Picosecond superconducting single-photon optical detector," *Appl. Phys. Lett.*, vol. 79, pp. 705-707, Aug. 2001.

[3] F. Marsili, F. Najafi, E. Dauler, F. Bellei, X. Hu *et al.*, "Single-Photon Detectors Based on Ultran arrow Superconducting Nanowires," *Nano Lett.*, vol. 11, pp. 2048-2053, Apr. 2011.

[4] A. Bezryadin, C. N. Lau, and M. Tinkham, "Quantum suppression of superconductivity in ultrathin nanowires," *Nature*, vol. 404, pp. , 971-974, Apr. 2000.

[5] A. Rogachev and A. Bezryadin, "Superconducting properties of polycrystalline Nb," *Appl. Phys. Lett.*, Vol. 83, pp. 512-514, Mar. 2003.

[6] H. Kim, S. Jamali, and A. Rogachev, "Superconductor-Insulator transition in long MoGe nanowires," Phys. Rev. Lett., vol. 109, pp. 027002 (1-5), Jul. 2012.

[7] C. N. Lau, N. Markovic, M. Bockrath, A. Bezryadin, and M. Tinkham, "Quantum phase slips in superconducting nanowires," *Phys. Rev. Lett.*, vol. 87, pp. 217003 (1-4), Nov. 2001.

[8] Y. Zhang and H. Dai, "Formation of metal nanowires on suspended single-walled carbon nanotubes," *Appl. Phys. Lett.*, vol. 77, pp. 3015-3017, Nov. 2000.

[9] I. L. Singer, R. N. Bolster, S. A. Wolf, and E.F. Skelton, " Abrasion resistance, microhardness and microstructures of single-phase niobium nitride films," *Thin Sol. Fil.*, vol. 107, pp. 207-215, Sep. 1983.

[10] K. Baba, R. Hatada , K. Udoh, and K. Yasuda, "Structure and properties of NbN and TaN films prepared by ion beam assisted deposition," *Nucl. Instr. Meth. Phys. Res. B*, vol. 127-128, pp. 841-845, May 1997.

[11] I. Hotovy, J. Huran, D. Buc, and R. Srnanek, "Thermal stablity of NbN films deposited on GaAs substrates," *Vac.*, vol. 50, pp. 45-48, May 1998.

[12] N. Giordano, "Evidence for macroscopic quantum tunneling in one-dimensional superconductors," *Phys. Rev. Lett.*, vol. 61, pp. 2137-2140, Apr. 1988.

[13] A. J. Van Run, J. Romijn, and J. E. Mooij, "Superconduction phase coherence in very weak aluminum strips," *Jpn. J. Appl. Phys.*, vol. 26, pp. 1765-1766, 1987.

[14] J. S. Penttila, U. Parts, P. J. Hakonen, M. A. Paalanen, and E. B. Sonin, ""Superconductor-insulator transition" in a single Josephson junction," Phys. Rev. Lett., vol. 82, pp. 1004-1007, Feb. 1999.

[15] K. Makise, T. Kawaguti and B. Shinozaki, "Superconductor-insulator transitions in quench-condensed Bi films on different underlayers," *Phys. E*, vol. 39, pp. 30-36, Jul. 2007.

[16] A. M. Goldman and Y. Liu, "The two-dimensional superconductor-insulator transition," Phys. D, vol. 83, pp. 163-177, May, 1995.

[17] M. Jung, H. Noh, Y. J. Doh, W. Song, Y. Chong *et al*., "Superconducting Junction of a Single-Crystalline Au Nanowire for an Ideal Josephson Device," *ACS Nano*, vol. 5, pp. 2271-2276, Feb. 2011.

[18] P. G. De Gennes, "Boundary Effects in Superconductors," *Rev. Mod. Phys.*, vol. 36, pp. 225–237, Jan.1964.

[19] P. G. De Gennes, "Superconductivity of Metals and Alloys," Addison-Wesley: Redwood City, CA, 1989.

[20] M. Octavio, M. Tinkham, G. E. Blonder, and T. M. Klapwijk, "Subharmonic Energy-Gap Structure in Superconducting Constrictions," *Phys. Rev. B*, vol. 28, pp. 6739–6746, Jun. 1983.

[21] M.Kemmler, M. Weides, M. Weiler, M. Opel, S. T. B. Goennenwein *et al.*, "Magnetic interference patterns in 0-π superconductor/ insulator/ ferromagnet/ superconductor Josephson junctions: Effects of asymmetry between 0 and π regions," *Phys. Rev. B*, vol. 81, pp. 054522 (1-8), Feb. 2010.